Pattern Recognition 123 (2022) 108313

Contents lists available at ScienceDirect

Pattern Recognition

journal homepage: www.elsevier.com/locate/patcog

Systematic generation of moment invariant bases for 2D and 3D tensor fields

Roxana Bujack[a,*], Xinhua Zhang[a], Tomáš Suk[b], David Rogers[a]

[a] Los Alamos National Laboratory, P.O. Box 1663, Los Alamos, NM 87545, USA
[b] Czech Academy of Sciences, Institute of Information Theory and Automation, Pod Vodárenskou věží 4, 182 08, Prague 8, Czech Republic

ARTICLE INFO

Article history:
Received 4 November 2020
Revised 16 July 2021
Accepted 9 September 2021
Available online 8 October 2021

Keywords:
Pattern detection
Rotation invariant
Moment invariants
Generator approach
Basis
Flexible
Vector
Tensor

ABSTRACT

Moment invariants have been successfully applied to pattern detection tasks in 2D and 3D scalar, vector, and matrix valued data. However so far no flexible basis of invariants exists, i.e., no set that is optimal in the sense that it is complete and independent for every input pattern.

In this paper, we prove that a basis of moment invariants can be generated that consists of tensor contractions of not more than two different moment tensors each under the conjecture of the set of all possible tensor contractions to be complete.

This result allows us to derive the first generator algorithm that produces flexible bases of moment invariants with respect to orthogonal transformations by selecting a single non-zero moment to pair with all others in these two-factor products. Since at least one non-zero moment can be found in every non-zero pattern, this approach always generates a complete set of descriptors.

1. Introduction

Pattern matching is a classical task on scalar data in image processing. Its generalization to higher dimensions enables application scientists working, for example, in hydrodynamics, continuum mechanics, plasma physics, environmental or space sciences, to detect patterns in their vector- and matrix-valued data, too. We treat all three of them simultaneously using the combined notion of tensor fields in 2D and 3D.

In many pattern detection applications, users want to find a pattern independent of the specific alignment of the provided template, but searching for every possible orientation of the template would cause a significant computational overhead and impair performance. In this paper we address this problem providing an optimal set of rotation-invariant descriptors, namely moment invariants. Moment invariants are capable of determining the degree of similarity between a given pattern template and its potentially rotated occurrence in the data by comparing only a single instance of the template [1]. Their building blocks, the moments, are the projections of a function to a function space basis. The similarity between a pattern and a field is inversely proportional to the Euclidean distance of their moments.

The moments themselves are not invariant w.r.t. rotation. There are two main approaches that turn them into moment invariants, i.e. that equip them with the power of orientation independence. First, normalization can be imagined as applying a transformation to the input pattern that places it into a predefined standard position. Second, the generator approach makes use of relations from algebra to find the right products, sums or other operations between the moments that result in invariants. The state of the art of both approaches makes use of tensor algebra, especially of tensor contractions to low ranks, because their transformations under rotations are simple.

Three properties are necessary to make an optimal set of descriptors: completeness, independence, and flexibility, Section 3.3. Theoretically the generator approach and normalization are equally powerful. Used optimally, they should be able to construct an optimal set of descriptors, but they each have their disadvantages. For example, to work optimally, the normalization requires contractions to first rank, which do not exist if all non-zero tensors happen to have even rank [2]. The currently best available generator approach [3] on the other hand requires the input pattern to have a non-zero first rank component, see Sections 4.1 and 4.2.

Long story short, there is currently no algorithm that produces a single flexible basis of 3D rotation-invariant descriptors even if

* Corresponding author.
E-mail addresses: bujack@lanl.gov (R. Bujack), xinhuazhang@lanl.gov (X. Zhang), suk@utia.cas.cz (T. Suk), dhr@lanl.gov (D. Rogers).

https://doi.org/10.1016/j.patcog.2021.108313
0031-3203/Published by Elsevier Ltd.

the data is only scalar-valued, let alone for vector- or matrix-fields. In this paper, we close this gap by presenting an algorithm that in precomputation generates an overcomplete set, which is complete for every possible pattern, together with a fast selection method that removes the superfluous, dependent elements for a given input pattern during runtime.

In the 2D case using complex moments, it has been shown that the optimal generator approach coincides with the optimal normalization approach [4]. It has been hypothesized that striving for these three criteria might also lead to the goal of unifying the generator and normalization approaches in 3D. That would result in a basis that combines the strengths of both approaches and beautifully tie the theory of moment invariant together.

The main contribution of this paper is the proof that it is possible to generate a basis of 2D and 3D moment invariants by only using tensor products with one or two different types of factors, contingent upon the conjecture of the set of all tensor contractions being complete, Section 5.1. This is a big step toward a unifying theory because a similar property is already known to be true for the 2D generator approach based on complex numbers [4] and the 2D and 3D normalization approaches [2].

This theoretical result has two advantages in practice, because on one hand it allows us to focus the search for bases to the small subgroup of products with only two factors and on the other hand it shows that and how a flexible basis can be generated for every possible pattern in 2D or 3D scalar-, vector-, or matrix-fields.

2. Related work

The first moment invariants were introduced to the image processing society by Hu [5]. Flusser [6] introduced the concept of a basis of moment invariants as a complete and independent set and presented a rule to generate a basis for any order for 2D scalar functions. Later, he proved that his basis also solves the inverse problem [7].

Schlemmer et al. [8,9] were the first to generalize the notion of moment invariants to 2D vector fields using the generator approach. Bujack et al. [10] followed the normalization approach and derived the first flexible basis of moment invariants for vector fields. Later, they unified the two approaches in 2D by showing that the flexible generator basis coincides with the flexible normalization basis.

For 3D functions, the task is much more challenging. One research path goes in the direction of the spherical harmonics. Lo and Don [11], Burel and Henocq [12], Kazhdan et al. [13], Canterakis [14], and Suk et al. [15] use them to construct moment invariants for 3D scalar functions. The resulting descriptors are usually not complete.

A second research path makes use of the tensor contraction method, as first used by Dirilten and Newman [16]. Pinjo, Cyganski, and Orr [17–19] use moment tensors to determine the orientation of scalar functions and to normalize with respect to linear transformations. All tensor contractions to zeroth rank are rotationally invariant, but there are infinitely many of them and it is difficult to find an independent set. Suk and Flusser [20] propose to calculate all possible zeroth rank contractions from moment tensors up to a given order and then skip the linearly dependent ones. Higher order dependencies still remain in their set.

Langbein and Hagen [3] also treat tensor fields of higher rank. They showed that the tensor contraction method can be generalized to arbitrary tensor fields and dimensions. They suggested an algorithm that is able to detect dependent invariants by means of linearly dependent derivatives. Independently, Hickman [21] suggests to use the derivatives, too. Gur and Johnson [22] contract tensors of the tensor field directly to derive invariants to outer rotation.

Table 1
State of the art of moment invariants for scalar, vector, and tensor fields. The parentheses indicate that this property is not proven, but a conjecture.

Approach	Dim.	Authors	Complete	Indep.	Flexible
Normalization	2D	Bujack, Hagen [2]	✓	✓	✓
Normalization	3D	Bujack, Hagen [2]	✓	✓	✓
Generator	2D	Bujack, Flusser [4]	✓	✓	✓
Generator	3D	Langbein, Hagen [3]	(✓)	✓	-

Bujack and Hagen follow the normalization approach, which provides the first complete and independent set that is also flexible w.r.t. vanishing moments for 3D tensor fields of arbitrary rank [2].

Please note that invariants can be constructed not only from moments of integer-valued orders, but also from fractional order moments [23,24] or from derivatives [25,26]. The fundamental theorem of moment invariants [27] guarantees that every algebraic invariant has a moment invariant counterpart.

The state of the art of the capabilities of moment invariant bases with respect to each of the two approaches and dimensions is summarized in Table 1. The definitions of complete, independent, and flexible can be found in Section 3.3.

In this paper, we will present the first algorithm to produce an independent and flexible basis for 3D functions using the generator approach. Like the algorithm by Langbein [3], it is complete if the Conjecture 1 holds.

3. Foundations

In this section, we will recap the theoretical underpinnings and notations of moment tensors. For both the normalization and the generator approaches, the most systematic and general framework to generate moment invariants of higher orders and for fields of higher field ranks, e.g., vector and matrix fields, is based on tensor calculus and makes use of the fact that contractions of high rank tensors are low rank tensors that are easy to handle.

3.1. Tensors and transformations

Tensors represent physical quantities that follow specific rules under transformations of the coordinate system. For a given basis, they can be represented as arrays of numbers. The rank of a tensor is the number of its indices with scalars having rank zero, vectors rank one, and matrices rank two. We refer the reader to introductions to tensor analysis [28,29].

Definition 1. A multidimensional array $T^{i_1\ldots i_n}_{j_1\ldots j_m}$ that, under an active transformation by the invertible matrix $A^i_j \in \mathbb{R}^{d\times d}$, behaves as:

$$T'^{i_1\ldots i_n}_{j_1\ldots j_m} = |\det(A^{-1})|^w A^{i_1}_{k_1}\ldots A^{i_n}_{k_n}(A^{-1})^{l_1}_{j_1}\ldots(A^{-1})^{l_m}_{j_m} T^{k_1\ldots k_n}_{l_1\ldots l_m}, \tag{1}$$

is called a (relative, axial) **tensor** of covariant rank m, contravariant rank n, and weight w. An (absolute) tensor has weight zero.

Lemma 1. *Let T and $\tilde{T}$ be two relative tensors of covariant rank m, contravariant rank n, and weight w and $\tilde{m}, \tilde{n}, \tilde{w}$ respectively.* Then the *product $T \otimes \tilde{T}$ (also called outer product or tensor product):*

$$(T\otimes\tilde{T})^{i_1\ldots i_n \tilde{i}_1\ldots\tilde{i}_{\tilde{n}}}_{j_1\ldots j_m \tilde{j}_1\ldots\tilde{j}_{\tilde{m}}} := T^{i_1\ldots i_n}_{j_1\ldots j_m}\tilde{T}^{\tilde{i}_1\ldots\tilde{i}_{\tilde{n}}}_{\tilde{j}_1\ldots\tilde{j}_{\tilde{m}}} \tag{2}$$

is a relative tensor of covariant rank $m+\tilde{m}$, contravariant rank $n+\tilde{n}$, and weight $w+\tilde{w}$.

Lemma 2. *Let T be a relative tensor of covariant rank m, contravariant rank n, and weight w.* Then the *contraction $T_{(i_k,j_l)}$ of a covariant index i_k and a contravariant index j_l*

$$T^{i_1\ldots i_{k-1}i_{k+1}\ldots i_n}_{j_1\ldots j_{l-1}j_{l+1}\ldots j_m\,(i_k,j_l)} := \sum_{\iota=1}^{d} T^{i_1\ldots i_{k-1}\iota i_{k+1}\ldots i_n}_{j_1\ldots j_{l-1}\iota j_{l+1}\ldots j_m} \tag{3}$$

is a relative tensor of covariant rank $m-1$, contravariant rank $n-1$, and weight w.

3.2. Moment tensors

Dirilten and Newman [16] arranged the moments of each order such that they obey the tensor transformation property (1) and use the contractions to generate moment invariants with respect to orthogonal transformations. Langbein et al. [3] generalized the definition of the moment tensor to tensor valued functions.

Definition 2. For a tensor field $T:\mathbb{R}^d \to \mathbb{R}^{d^n \times d^m}$ with compact support, the **moment tensor** ${}^oM$ of order $o \in \mathbb{N}$ takes the shape

$$ {}^oM^{i_1\ldots i_n k_1\ldots k_o}_{j_1\ldots j_m} := \int_{\mathbb{R}^d} x^{k_1}\ldots x^{k_o} T^{i_1\ldots i_n}_{j_1\ldots j_m}(x)\,\mathrm{d}^d x. \tag{4}$$

The following theorem and corrolary are the foundation of the generator approach in 3D because they show that all zeroth rank contractions are moment invariants. Proofs can be found in the work by Bujack and Hagen [2].

Theorem 1. *The moment tensor of order o of a tensor field of covariant rank m, contravariant rank n, and weight w is a tensor of covariant rank m, contravariant rank $n+o$ and weight $w-1$.*

Corollary 1. *The rank zero contractions of any product of the moment tensors are moment invariants with respect to rotation and reflection.*

We will distinguish between **homogeneous invariants**, which are constructed from only a single moment tensor M and its powers, and **simultaneous invariants**, or mixed invariants, which contain more than one kind of moment tensors.

3.3. Desirable properties of a set of descriptors

Corollary 1 provides an infinite number of invariants, with most of them containing redundant information. In order to optimally describe a function, a set of moment invariants should have the following three desirable qualities [4]:

Completeness: The set is called complete if any moment invariant can be constructed from it. This property guarantees that any two objects that differ by something other than a rotation/reflection can be discriminated.

Independence: The set is independent if none of its elements can be constructed from the other elements. This property makes sure that the number of descriptors is minimal.

Flexibility: The set is flexible, also called existent, if it is generally defined and complete without requiring any specific moments to be non-zero. This property ensures that the set can detect and discriminate any pattern independent of its specific form.

4. Langbein's algorithm

Removing dependent contractions has long been a difficult task until independently Langbein and Hagen [3] and Hickman [21] suggested to test the derivatives of the invariants for linear dependence in order to find polynomial dependencies in the invariants themselves.

The former suggest this seminal algorithm to test the dependence, which we will call Langbein's algorithm in this paper. We provide a short overview. Details can be found in the original paper [3].

1. Initiate all moment tensors up to a given order $o_{\max}$ with random numbers.
2. Compute all zeroth rank contractions of all their products up to a given maximum number of factors $p_{\max}$.
3. Compute their derivatives w.r.t. all moments up to $o_{\max}$.
4. Build a matrix with as many rows as moments.
5. Until the number of maximally possible invariants is achieved: add the next derivative to the matrix if it increases the matrix's rank.

Langbein and Hagen [3] state that the order in which the invariants are tested is with increasing number of factors $p \le p_{\max}$, but not how the order is within each group of equal factors. We assume that within each group, we sort alphabetically first by moment order in the product, e.g., ${}^2M^{23}M$ comes before ${}^2M^3M^2$, and then by contraction index, e.g., (0,1),(2,3) comes before (0,2),(1,3). Because of commutativity, we only consider products of increasing moment order and contractions of increasing indices. When invariance w.r.t. translation and scaling is needed in an application, typically the zeroth and first moments are normalized and do no longer contain information that can be used to construct rotation invariants[1]. Please note that we include them in this paper for brevity even though Langbein and Hagen originally excluded them in their work. All treated algorithms function with and without them.

4.1. 2D Example of non-flexibility

Langbein's Algorithm generates a basis of moment invariants, but it is not flexible. We will show this using a 2D scalar pattern. Up to order 3, Langbein's algorithm returns the following basis.

$$ {}^0M,\ {}^2M_{(0,1)},\ {}^1M^2{}_{(0,1)},\ {}^1M^3M_{(0,1),(2,3)},\ {}^2M^2{}_{(0,2),(1,3)},\ {}^1M^{22}M_{(0,2),(1,3)},\ {}^3M^2{}_{(0,1),(2,3),(4,5)},\ {}^3M^2{}_{(0,3),(1,4),(2,5)},\ {}^1M^2M^3M_{(0,3),(1,4),(2,5)}. \tag{5}$$

For purely quadratic and cubic patterns, the only non-vanishing invariants are

$$\begin{aligned} {}^2M_{(0,1)} &= M_{00}+M_{11}\\ {}^2M^2{}_{(0,2),(1,3)} &= M_{00}^2+2M_{01}^2+M_{11}^2\\ {}^3M^2{}_{(0,1),(2,3),(4,5)} &= M_{000}^2+M_{001}^2+M_{011}^2+M_{111}^2+\ 2M_{000}M_{011}\\ &\quad +2M_{001}M_{111}\\ {}^3M^2{}_{(0,3),(1,4),(2,5)} &= M_{000}^2+3M_{001}^2+3M_{011}^2+M_{111}^2. \end{aligned} \tag{6}$$

This basis is not complete for the function shown in Fig. 1

$$ f(x,y) = (80x^3+48xy^2-48x+18x^2+6y^2-6)/\pi\,\chi(x^2+y^2\le 1), \tag{7}$$

with χ corresponding to the characteristic function. It has the moments

$$ M_{11} \quad = 1, \quad M_{000} \quad = 1, \tag{8}$$

and all other moments up to order 3 are zero. Especially, there is no linear component. The values of the non-vanishing invariants of Langbein's basis are

$$\begin{aligned} {}^2M_{(0,1)} &= 1, & {}^2M^2{}_{(0,2),(1,3)} &= 1\\ {}^3M^2{}_{(0,1),(2,3),(4,5)} &= 1, & {}^3M^2{}_{(0,3),(1,4),(2,5)} &= 1. \end{aligned} \tag{9}$$

We can determine that the zeroth and first order moments are all zero from the vanishing invariants, but then we have four equations left to reconstruct $3+4-1=6$ remaining degrees of freedom, which consist of the moments of orders 2 and 3 minus one DoF for the rotational invariance. Clearly we cannot reconstruct them, which shows that the set (5) is not complete for this pattern (7).

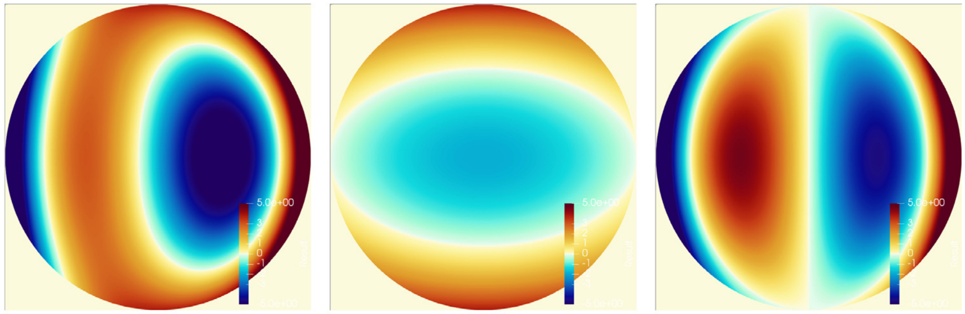

The function $(80x^3 + 48xy^2 - 48x + 18x^2 + 6y^2 - 6)/\pi$. Its quadratic part $(18x^2 + 6y^2 - 6)/\pi$. Its cubic part $(80x^3 + 48xy^2 - 48x)/\pi$.

Fig. 1. The function from Eq. (7) and its components visualized using colormapping. Langbein's basis is not complete for this pattern.

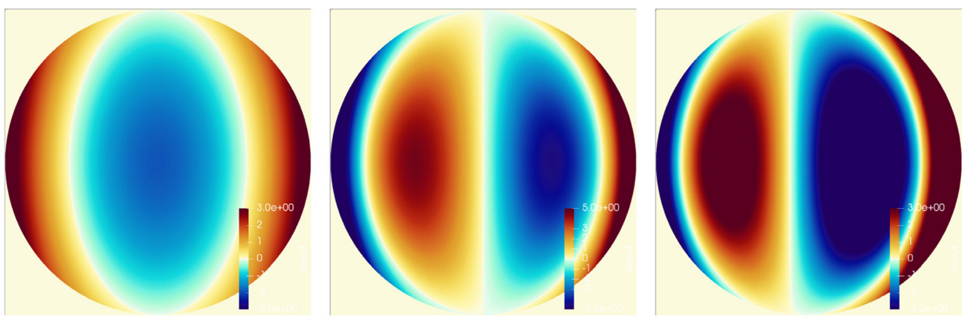

Quadratic part $(18y^2 + 6x^2 - 6)/\pi$. Cubic part $(80x^3 + 48xy^2 - 48x)/\pi$. The function $(80x^3 + 48xy^2 - 48x + 18y^2 + 6x^2 - 6)/\pi$.

Fig. 2. The function (10) and its components visualized using colormapping. Even though the function differs clearly from Eq. (7), the Langbein invariants are identical (9).

This lack of completeness can especially lead to false positives. For example, the function

$$f(x, y) = (80x^3 + 48xy^2 - 48x + 18y^2 + 6x^2 - 6)/\pi\, \chi(x^2 + y^2 \le 1), \tag{10}$$

shown in Fig. 2, has the moments

$$M_{00} = 1, \quad M_{000} = 1. \tag{11}$$

All other moments up to order 3 are zero. The values of the invariants are identical to the ones (9) of the first function (7), and therefore the Langbein basis cannot distinguish between them and would produce false positives.

4.2. 3D Example of non-flexibility

Langbein's basis for 3D scalar functions up to order 3 contains the elements

$$\begin{gathered}
{}^0M, {}^2M_{(0,1)}, {}^1M^2{}_{(0,1)}, {}^1M^3M_{(0,1),(2,3)}, {}^2M^2{}_{(0,2),(1,3)}, {}^3M^2{}_{(0,1),(2,3),(4,5)},\\
{}^3M^2{}_{(0,3),(1,4),(2,5)}, {}^1M^{22}M_{(0,2),(1,3)}, {}^1M^2M^3M_{(0,1),(2,3),(4,5)},\\
{}^1M^2M^3M_{(0,3),(1,4),(2,5)}, {}^2M^3{}_{(0,2),(1,4),(3,5)}, {}^2M^{13}M^2{}_{(0,2),(1,3),(4,5),(6,7)},\\
{}^2M^{13}M^2{}_{(0,2),(1,5),(3,4),(6,7)}, {}^2M^{13}M^2{}_{(0,2),(1,5),(3,6),(4,7)}, {}^1M^{33}M_{(0,3),(1,4),(2,5)},\\
{}^1M^{23}M^2{}_{(0,2),(1,3),(4,5),(6,7)}, {}^1M^{23}M^2{}_{(0,2),(1,5),(3,6),(4,7)}
\end{gathered} \tag{12}$$

Especially, for a purely cubic function, all invariants are zero except for

$$\begin{aligned}
{}^3M^2{}_{(0,1),(2,3),(4,5)} &= M_{000}^2 + M_{001}^2 + M_{011}^2 + M_{111}^2 + M_{002}^2 + M_{112}^2 + M_{022}^2\\
&\quad + M_{122}^2 + M_{222}^2 + 2M_{000}M_{011} + 2M_{000}M_{022}\\
&\quad + 2M_{001}M_{111} + 2M_{001}M_{122} + 2M_{011}M_{022} + 2M_{111}M_{122}\\
&\quad + 2M_{002}M_{112} + 2M_{002}M_{222} + 2M_{112}M_{222}\\
{}^3M^2{}_{(0,3),(1,4),(2,5)} &= M_{000}^2 + 3M_{001}^2 + 3M_{011}^2 + M_{111}^2 + 3M_{002}^2\\
&\quad + 6M_{012}^2 + 3M_{112}^2 + 3M_{022}^2 + 3M_{122}^2 + M_{222}^2
\end{aligned} \tag{13}$$

We can deduce that the moments up to rank 2 are all zero, but then we are left with only two equations to reconstruct $10 - 3 = 7$ degrees of freedom corresponding to the independent moments of order 3 minus the 3 DoF for the 3D rotation, which shows that Langbein's basis is not flexible.

Especially, the two functions

$$\begin{aligned}
f_1(x, y, z) &= \Big(\frac{25}{4}x^3 + \frac{9}{4}x^2y + \frac{9}{4}x^2z + \frac{15}{4}xy^2 + xyz + \frac{15}{4}xz^2 + \frac{3}{4}y^3 + \frac{3}{4}y^2z\\
&\quad + \frac{3}{4}yz^2 + \frac{3}{4}z^3 - \frac{15}{4}x - \frac{3}{4}y - \frac{3}{4}z\Big)\chi(x^2 + y^2 + z^2 \le 1) f_2(x, y, z)\\
&= \Big(\frac{25}{4}x^3 + \frac{9}{4}x^2y + \frac{9}{4}x^2z + \frac{15}{4}xy^2 - xyz + \frac{15}{4}xz^2 + \frac{3}{4}y^3\\
&\quad + \frac{3}{4}y^2z + \frac{3}{4}yz^2 + \frac{3}{4}z^3 - \frac{15}{4}x - \frac{3}{4}y - \frac{3}{4}z\Big)\chi(x^2 + y^2 + z^2 \le 1)
\end{aligned} \tag{14}$$

in Fig. 3 have the moments

$$\begin{aligned}
M_{000} &= 1, & M_{001} &= 1, & M_{002} &= 1, & M_{012} &= 1,\\
M_{000} &= 1, & M_{001} &= 1, & M_{002} &= 1, & M_{012} &= -1,
\end{aligned} \tag{15}$$

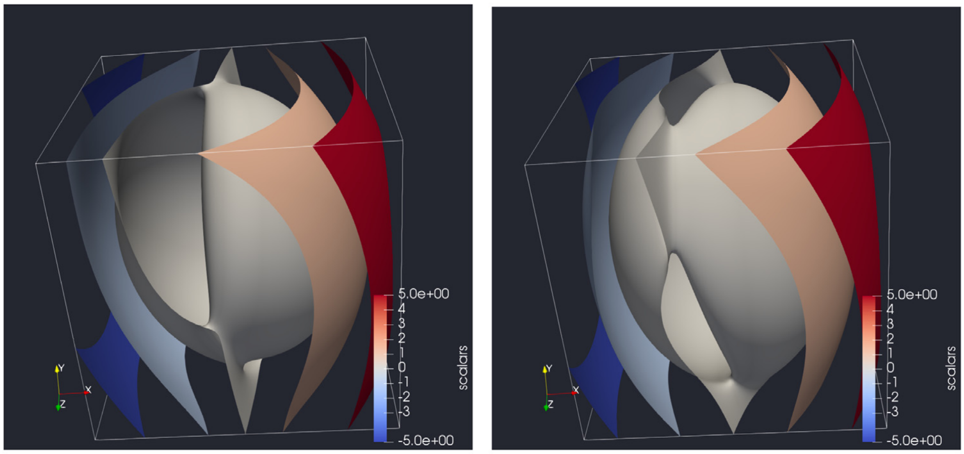

The function f_1 from (14). The function f_2 from (14).

Fig. 3. The two functions from (14) cannot be distinguished by Langbein's basis.

with all other moments up to order 3 being zero. They cannot be discriminated by Langbein's basis because they both satisfy

$$ {}^{3}M^{2}{}_{(0,1),(2,3),(4,5)} = 3, \quad {}^{3}M^{2}{}_{(0,3),(1,4),(2,5)} = 13, \tag{16} $$

with all other invariants being zero.

4.3. Analysis of the problem with flexibility

The origin of the problem lies in the fact that independence and completeness are properties that do not fully translate from their theoretical, analytic forms to their evaluations using certain random numbers. A set of invariants can be independent for one configuration while being dependent for another.

Our first idea was to run Langbein's algorithm with the moments of the input pattern instead of random numbers, but that did not work.

For example, run with the moments of the input function (7), Langbein's algorithm would classify the simultaneous invariants of orders 2 and 3 as dependent w.r.t. the previously added homogeneous invariants of orders 2 and 3. That means it is discarded even though we will see that one of them contains new information in Section 5.5.

Also, it would make the method computationally prohibitive if the whole algorithm would have to be run every single time a pattern is searched. We have to find a method to precompute independent invariants.

The examples in Sections 4.1 and 4.2 highlight that the problem of non-flexibility comes from the simultaneous invariants, because they lose their information content if one of the involved tensors vanishes. The more different factors appear in the invariant, the larger the set of patterns becomes for which it becomes useless. In the next section, we will analyze how we can reduce the number of factors and specifically select the kind of factors in the simultaneous invariants to avoid this problem.

5. Systematic generation of bases of moment invariants

In this section, we will systematically analyze the numbers of degrees of freedom and invariants and show that it is possible to generate bases that consist of homogeneous invariants and simultaneous invariants with no more than two different factors. A summary can be found in Tables 2 and 3.

One result is that for each pattern, there exists a complete set of rotation invariants if the set of all tensor contractions is complete in the first place and we will show how to derive it.

Table 2
Summary of the numbers of independent moments of order o and field rank r_f from Lemmata 3 and 7 and independent invariants of that order from Lemmata 4 and 8. The values are correct for ranks $r = r_f + o > 1$. For low rank exceptions, please refer to the lemmata.

Dim.	r_f	ind. moments	ind. invariants
2D	0	$o+1$	o
	1	$2(o+1)$	$2o+1$
	2	$4(o+1)$	$4o+3$
3D	0	$\frac{1}{2}(o+1)(o+2)$	$\frac{1}{2}(o+1)(o+2)-3$
	1	$\frac{3}{2}(o+1)(o+2)$	$\frac{3}{2}(o+1)(o+2)-3$
	2	$\frac{9}{2}(o+1)(o+2)$	$\frac{9}{2}(o+1)(o+2)-3$

We have seen in the motivating examples in Sections 4.1 and 4.2 that products of moment tensors lose their information if one of the factors is zero. We therefore want to construct bases from products that have the least amount of factors. The structures of Sections 5.2 and 5.3 are identical. We will first compute the number of independent invariants up to a given order, i.e. the number of descriptors we have to find (column 3 in Table 3). Then we start filling these slots with homogeneous invariants (column 4 in Table 3). Since they have only one factor, they never lose their information through a multiplication with zero. The difference is the number of simultaneous invariants that are needed to complete the set (column 5 in Table 3). Every pattern that is not identically zero has one non-zero moment tensor. If we can fill these remaining slots with products pairing only this non-zero tensor with each other tensor, then we can avoid the information loss that comes from multiplications with zero altogether. Exactly this is the result of Theorem 3 in 2D and Theorem 5 in 3D.

5.1. Conjecture

Like all tensor contraction-based algorithms, our algorithm is based on the following conjecture.

Conjecture 1. *The set of all contractions of a moment tensor to zeroth order are a complete set of rotation/reflection invariants of the corresponding moments.*

We are not able to prove this property, but we could show that it holds up to rank 6 in 2D and rank 4 in 3D, which can be seen in the appendix.

Table 3
Summary of the numbers of independent invariants up to order o_m and of field rank r_f from Lemmata 5 and 9, the number of independent homogenous invariants up to that order and their difference, i.e. the number of simultaneous invariants that need to be added from Lemmata 6 and 10. The values are correct for ranks $r = r_f + o_m > 1$. For low rank exceptions, please refer to the lemmata.

Dim.	r_f	ind. invariants	ind. hom. invariants	diff.
2D	0	$\frac{1}{2}(o_m+1)(o_m+2)-1$	$\frac{1}{2}o_m(o_m+1)$	o_m-1
	1	$(o_m+1)o(o_m+2)-1$	$(o_m+1)^2$	o_m
	2	$2(o_m+1)o(o_m+2)-1$	$(o+1)(2o+3)$	o_m
3D	0	$\frac{1}{6}(o_m+1)(o_m+2)o(o_m+3)-3$	$\frac{1}{6}(o_m^3+6o_m^2-7o_m)+2$	$3o_m-4$
	1	$\frac{1}{2}(o_m+1)(o_m+2)o(o_m+3)-3$	$\frac{1}{2}(o_m^3+6o_m^2+5o_m+2)$	$3o_m-1$
	2	$\frac{3}{2}(o_m+1)(o_m+2)o(o_m+3)-3$	$\frac{3}{2}(o_m+1)^2(o_m^2+4)$	$3o_m$

5.2. Number of independent invariants in 2D

We will first look at tensor fields of arbitrary rank in 2D and show that up to a maximal order $o_m \in \mathbb{N}$ a basis can be formed from the homogeneous invariants plus one simultaneous invariant for each combination of one designated order o_0 with all other orders $o_i \leq o_m$.

Lemma 3 (Independent moments)**.** *The number of independent moments of a moment tensor of order $o \geq 0$ of a two-dimensional function with field-rank $r_f \geq 0$ is $2^{r_f}(o+1)$.*

Proof. A two-dimensional order o moment tensor $T^{k_1,\dots,k_o}$ of a function with field-rank zero $r_f = 0$, i.e., a scalar field, is symmetric. We can see from (4) that the number of independent entries is identical to the different ways of assigning 0 or 1 in ascending order to the indices $k_1,\dots,k_o$. This can be encoded as the first appearance of 1, for which there are $o+1$ options, i.e., any of the indices plus the option of it not appearing at all, i.e.,

$$1 + \sum_{i=1}^{o} 1 = o+1. \tag{17}$$

For any dimension $d > 0$, functions with higher field-rank, e.g., a vector field with $r_f = 1$ or a matrix field with $r_f = 2$, have d^{r_f} components. Multiplication with the degrees of freedom in each of their components completes the proof. □

Lemma 4 (Independent hom. invariants)**.** *The number of independent homogeneous invariants of a 2D moment tensor of rank $r = o + r_f > 0$ with order $o \geq 0$ and field-rank $r_f \geq 0$ is $2^{r_f}(o+1) - 1$.*

For $r = o + r_f = 0$, there is 1 homogeneous invariant.

Proof. The generation of any kind of invariance discards the number of degrees of freedom of the transformation w.r.t. which the invariance is achieved. Therefore, the number of possible independent invariants is the number of independent moments minus the degrees of freedom of a rotation.

Now the assertion follows from Lemma 3 and the fact that a two-dimensional rotation has one degree of freedom.

The exception $r = 0$ comes from the fact that a zeroth rank tensor is invariant to orthogonal transformations. □

Lemma 5 (Independent invariants)**.** *The number of independent invariants of all 2D moments up to order $o_m \geq 0$ of a function with field-rank $r_f \geq 0$ is $2^{r_f}(o_m+1)(o_m+2)/2 - 1$.*

For order $o_m = 0$, there is 1 independent invariant.

Proof. Analogous to the proof of Lemma 4, the number of possible independent invariants is the number of independent moments minus the degrees of freedom of a rotation.

We can see from Lemma 3 and straight calculation that the number of independent moments up to order o_m is

$$\sum_{o=0}^{o_m} 2^{r_f}(o+1) = 2^{r_f}(o_m+1)(o_m+2)/2. \tag{18}$$

Again the main assertion follows from Lemma 3 and the fact that a two-dimensional rotation has one degree of freedom.

Finally the exception $o_m = 0$ follows again because a zeroth rank tensor is invariant. □

Lemma 6 (Simultaneous invariants)**.** *If we use all homogeneous invariants for a 2D function with field-rank $r_f > 0$, we need to add o_m simultaneous invariants to get to the total number of independent invariants.*

For $r_f = 0$, i.e., scalar fields, we need to add $o_m - 1$ simultaneous invariants.

Proof. It follows from Lemma 4 that for 2D fields with $r_f > 0$, the number of independent homogeneous invariants up to order o_m is

$$\sum_{o=0}^{o_m} 2^{r_f}(o+1) - 1 = (o_m+1)(2^{r_f}(o_m+2)-2)/2. \tag{19}$$

Lemma 5 shows that the difference between independent invariants and independent homogeneous invariants is

$$(o_m+1)(o_m+2)/2 - 1 - (o_m+1)(2^{r_f}(o_m+2)-2)/2 = o_m. \tag{20}$$

For 2D scalar fields, i.e., $r_f = 0$, Lemma 4 shows that the number of independent homogeneous invariants up to order o_m is composed of adding up $2^0(o+1) - 1$ for all $o > 0$ plus 1 for $o = 0$, i.e.,

$$1 + \sum_{o=1}^{o_m} o = o_m(o_m+1)/2 + 1. \tag{21}$$

From Lemma 5, we can then see that the difference between independent invariants and independent homogeneous invariants is

$$(o_m+1)(o_m+2)/2 - 1 - (o_m(o_m+1)/2 + 1) = o_m - 1. \tag{22}$$

□

Theorem 2 (Overcomplete set)**.** *For 2D and the maximum order $o_m > 0$, the smallest set that is always able to discriminate two functions that differ by more than an orthogonal transformation has $(o_m+1)(2^{r_f}o_m + o_m + 2^{r_f+1} - 2)/2$ elements if $r_f > 0$.*

For $r_f = 0$, i.e., scalar fields, the smallest set has $o_m^2 + 1$ elements.

Proof. For $r_f > 0$, taking the $2^{r_f}(o+1) - 1$ homogeneous invariants from Lemma 4 plus the one simultaneous invariant for all combinations of orders o_i, o_j results in

$$\sum_{o=0}^{o_m}(2^{r_f}(o+1)-1) + \sum_{o_i=0}^{o_m}\sum_{o_j=o_1+1}^{o_m} 1 = (o_m+1)(2^{r_f}o_m + o_m + 2^{r_f+1} - 2)/2. \tag{23}$$

For $r_f = 0$, taking the $2^{r_f}(o+1) - 1$ homogeneous invariants from Lemma 4 for $r = o + r_f > 1$ plus the one simultaneous invariant for all combinations of orders $o_i, o_j > 1$ results in

$$\sum_{o=1}^{o_m}((o+1)-1) + \sum_{o_i=1}^{o_m}\sum_{o_j=o_1+1}^{o_m} 1 = o_m^2 + 1. \tag{24}$$

□

Theorem 3 (Flexible basis). *For 2D and any given order $o_0 \le o_m$ with $r_f + o_0 > 0$, we can find a complete and independent basis using all homogeneous invariants up to order o_m and one simultaneous invariant for each combination of o_0 and o with $r = r_f + o > 0$.*

Proof. We know from Lemma 3 that the number of independent moments between order o_0 plus o is $2^{r_f}(o_0+1) + 2^{r_f}(o+1) = 2^{r_f}(o_0+o+2)$ and from Lemma 4 for $r = o + r_f > 1$ that the number of homogeneous invariants between these orders is $2^{r_f}(o_0 + 1) - 1 + 2^{r_f}(o+1) - 1 = 2^{r_f}(o_0+o+2) - 2$. Considering that the degrees of freedom of a rotation in 2D is one, there exists one independent simultaneous invariant because $2^{r_f}(o_0+o+2) - (2^{r_f}(o_0+o+2) - 2) - 1 = 1$.

Therefore the number of simultaneous invariants that contain o_0 are

$$\sum_{o_0 \neq o=1}^{o_m} 1 = o_m - 1, \tag{25}$$

which coincides with the number needed from Lemma 6. □

5.3. Number of independent invariants in 3D

Now we will analyze the independent invariants of tensor fields of arbitrary rank in 3D and show that up to a maximal order o_m, a basis can be formed from the homogeneous invariants plus three simultaneous invariants for each combination of one designated order o_0 with all other orders $o_i < o_m$. This section follows the same structure as the previous one.

Lemma 7 (Independent moments). *The number of independent moments of a moment tensor of order $o \ge 0$ of a 3D function with field-rank $r_f \ge 0$ is $3^{r_f}(o+1)(o+2)/2$.*

Proof. A 3D order o moment tensor $T^{k_1,\dots,k_o}$ of a function with field-rank zero $r_f = 0$, i.e., a scalar field, is symmetric. We can see from (4) that the number of independent entries is identical to the different ways of assigning 0, 1, or 2 in ascending order to the indices $k_1, \dots, k_o$. This can be encoded through the first appearance of 1 and the first appearance of 2. Let the first appearance of 1 occur at index k_i with $i = 1, \dots, o$, then the possible locations for the first appearance of 2 range from $i+1$ to o. This results in

$$\sum_{i=1}^{o}\sum_{j=i+1}^{o} 1 = \frac{o^2 - o}{2} \tag{26}$$

degrees of freedom if both appear, plus

$$2\sum_{j=1}^{o} 1 = 2o \tag{27}$$

if only one of them appears, plus 1 if neither appear. From straight calculation follows that we have $(o^2 - o)/2 + 2o + 1 = (o+1)(o+2)/2$ independent moments.

For any dimension $d > 0$, functions with higher field-rank, e.g., a vector field with $r_f = 1$ or a matrix field with $r_f = 2$, have d^{r_f} components. Multiplication with the degrees of freedom in each of their components completes the proof. □

Lemma 8 (Independent hom. invariants). *The number of 3D independent homogeneous invariants of a moment tensor of rank $r = o + r_f > 1$ with order $o \ge 0$ and field-rank $r_f \ge 0$ is $3^{r_f}(o+1)(o+2)/2 - 3$.*

For each $0 \le r = o + r_f \le 1$, there is 1 homogeneous invariant.

Proof. The generation of any kind of invariance discards the number of degrees of freedom of the transformation w.r.t. which the invariance is achieved. Therefore, the number of possible independent invariants is the number of independent moments minus the degrees of freedom of a rotation.

Now the assertion follows from Lemma 7 and the fact that a 3D rotation has three degrees of freedom.

The exceptions $0 \le r \le 1$ come from the fact that a zeroth rank tensor and the Euclidean norm of a first rank tensor are invariants to orthogonal transformations. □

Lemma 9 (Independent invariants). *The number of independent invariants of all moments up to order $o_m > 0$ of a function with field-rank $r_f \ge 0$ is $3^{r_f}(o_m+1)(o_m+2)(o_m+3)/6 - 3$.*

Up to order $o_m = 0$, there is 1 and for $o_m = 1$, there are 2 independent invariants.

Proof. Analogous to the proof of Lemma 8, the number of possible independent invariants is the number of independent moments minus the three degrees of freedom of a rotation.

For $o > 1$, Lemma 7 shows that the number of independent moments up to order o_m is

$$\sum_{o=0}^{o_m} 3^{r_f}(o_m+1)(o_m+2)/2 = 3^{r_f}(o_m+1)(o_m+2)(o_m+3)/6. \tag{28}$$

The exceptions $0 \le o \le 1$ follow again because a zeroth rank tensor and the Euclidean norm of a first rank tensor are invariants. □

Lemma 10 (Simultaneous invariants). *If we use all homogeneous invariants for a 3D function with field-rank $r_f > 1$, we need to add $3o_m$ simultaneous ones to get to the total number of independent invariants.*

For $r_f = 1$, we need $3o_m - 1$ and for $r_f = 0$, we need $3o_m - 4$ simultaneous invariants.

Proof. For $r_f > 1$, the exception $r \le 1$ in Lemma 8 cannot occur and the number of independent moments up to order o_m is

$$\sum_{o=0}^{o_m} 3^{r_f}(o+1)(o+2)/2 - 3 = ((o_m+1)(3^{r_f}(o_m^2 + 5o_m^2) + 6) - 18)/6. \tag{29}$$

The difference to the total number of invariants from Lemma 9 results in

$$\begin{aligned} &3^{r_f}(o_m+1)(o_m+2)(o_m+3)/6 - 3 \\ &\quad -((o_m+1)(3^{r_f}(o_m^2 + 5o_m^2) + 6) - 18)/6 = 3o_m. \end{aligned} \tag{30}$$

For $r_f = 1$, i.e., vector fields, we know from Lemma 8 that the number of independent homogeneous invariants up to order $o_m \ge 0$ is given through summing over 1 for $o_m = 0$ and $3^1(o+1)(o+2)/2 - 3$ for $o_m > 0$, i.e.,

$$1 + \sum_{o=1}^{o_m} 3(o+1)(o+2)/2 - 3 = (o_m^3 + 6o_m^2 + 5o_m + 2)/2. \tag{31}$$

The difference to the total number of invariants from Lemma 9 results in

$$3^{r_f}(o_m+1)(o_m+2)(o_m+3)/6 - 3 - (o_m^3 + 6o_m^2 + 5o_m + 2)/2 = 3o_m - 1 \tag{32}$$

and for $o_m = 0$, we do not need any simultaneous invariants.

For $r_f = 0$, i.e., scalar fields using Lemma 8, we know that the number of independent homogeneous invariants up to order $o_m > 1$ is given through summing over 1 for $o_m \leq 1$ and $3^0(o+1)(o+2)/2 - 3$ for $o_m > 1$, i.e.,

$$1 + 1 + \sum_{o=2}^{o_m} 3^{r_f}(o+1)(o+2)/2 - 3 = o_m(o_m - 1)(o_m + 7)/6 + 2. \tag{33}$$

Trivially for $o_m = 0$, we have 1 and for $o_m = 1$, we have 2. Again Lemma 9 shows that the difference between independent invariants and independent homogeneous invariants up to $o_m > 1$ is

$$(o_m + 1)(o_m + 2)(o_m + 3)/6 - (o_m(o_m - 1)(o_m + 7)/6 + 2) = 3o_m - 4 \tag{34}$$

and for $o_m \leq 1$, we do not need any simultaneous invariants. □

Theorem 4 (Overcomplete set)**.** *For 2D and the maximum order $o_m > 0$ the smallest set that is always able to discriminate two functions that differ by more than an orthogonal transformation has $(o_m^3 + 15o_m^2 - 22o_m + 18)/6$ elements if $r_f = 0$, $(o_m^3 + 9o_m^2 + 6o_m + 2)/2$ elements if $r_f = 1$, and $3/2(o_m + 1))(o_m^2 + 6o_m + 4)$ elements if $r_f > 1$.*

Proof. For $r_f > 1$, the number of simultaneous invariants is given through

$$\sum_{o_i=0}^{o_m} \sum_{o_j=o_i+1}^{o_m} 3 = 3/2o_m(o_m + 1). \tag{35}$$

Adding the number of independent homogeneous invariants from the proof of Lemma 10 leads to

$$\begin{aligned} &3/2o_m(o_m + 1) + (o_m + 1)(3^{r_f}(o_m^2) + 5o_m^2) + 6) - 18)/6 \\ &= 3/2(o_m + 1))(o_m^2 + 6o_m + 4). \end{aligned} \tag{36}$$

For $r_f = 1$, i.e., vector fields, the number of simultaneous invariants is given through

$$\sum_{o=1}^{o_m} 2 + \sum_{o_i=1}^{o_m} \sum_{o_j=o_i+1}^{o_m} 3 = 1/2o_m(3o_m + 1). \tag{37}$$

Adding the number of independent homogeneous invariants from the proof of Lemma 10 leads to

$$1/2o_m(3o_m + 1) + (o_m^3 + 6o_m^2 + 5o_m + 2)/2 = (o_m^3 + 9o_m^2 + 6o_m + 2)/2. \tag{38}$$

For $r_f = 0$, i.e., scalar fields, the number of simultaneous invariants is given through

$$\sum_{o=2}^{o_m} 2 + \sum_{o_i=2}^{o_m} \sum_{o_j=o_i+1}^{o_m} 3 = (o_m - 1)(3o_m - 2)/2. \tag{39}$$

Adding the number of independent homogeneous invariants from the proof of Lemma 10 leads to

$$\begin{aligned} &(o_m - 1)(3o_m - 2)/2 + o_m(o_m - 1)(o_m + 7)/6 + 2 \\ &= (o_m^3 + 15o_m^2 - 22o_m + 18)/6. \end{aligned} \tag{40}$$

□

Theorem 5 (Flexible basis)**.** *For 3D and any given order $o_0 \leq o_m$ with $r_0 = r_f + o_0 > 1$, we can find a complete and independent basis using all homogeneous invariants up to order o_m and three simultaneous invariants for each combination of o_0 and o with $r = r_f + o > 1$ and two simultaneous invariants for the combination of o_0 and o with $r = r_f + o = 1$.*

Proof. We know from Lemma 7 that the number of independent moments of order o_0 is $3^{r_f}(o_0 + 1)(o_0 + 2)/2$ and of order o is $3^{r_f}(o + 1)(o + 2)/2$ and from Lemma 8 that the numbers of corresponding homogeneous invariants are $3^{r_f}(o_0 + 1)(o_0 + 2)/2 - 3$ and $3^{r_f}(o + 1)(o + 2)/2 - 3$ for $r = o + r_f > 1$. Considering that the degrees of freedom of a rotation in 3D is three, we know that there exist three independent simultaneous invariants because $3^{r_f}(o_0 + 1)(o_0 + 2)/2 + 3^{r_f}(o + 1)(o + 2)/2 - (3^{r_f}(o_0 + 1)(o_0 + 2)/2 - 3 + 3^{r_f}(o + 1)(o + 2)/2 - 3) - 3 = 3$.

If $r_f > 1$, all $r = o + r_f > 1$ and therefore the number of simultaneous invariants that contain o_0 are

$$\sum_{o_0 \neq o=0}^{o_m} 3 = 3o_m, \tag{41}$$

If $r_f = 1$, we have $r = o + r_f = 1$ for $o = 0$ and therefore the number of simultaneous invariants that contain o_0 are

$$\sum_{o_0 \neq o=1}^{o_m} 3 + 2 = 3(o_m - 1) + 2 = 3o_m - 1 \tag{42}$$

If $r_f = 0$, we have $r = o + r_f = 1$ for $o = 1$ and therefore the number of simultaneous invariants that contain o_0 are

$$\sum_{o_0 \neq o=2}^{o_m} 3 + 2 = 3(o_m - 2) + 2 = 3o_m - 4. \tag{43}$$

All three cases coincide with the number needed from Lemma 10, which completes the proof. □

5.4. Algorithm

Our algorithm follows the main idea from Bujack et al. [4]. In a nutshell, we will first use all possible independent homogeneous invariants and then add simultaneous invariants between the lowest order tensor that is significantly different from zero ${}^{o_0}M >> 0$ paired with all other tensors.

Explicitly for a given maximum order o_m, we precompute the overcomplete set of invariants from Theorems 2 and 4 that contains all homogeneous invariants and for each pair of moments $o_i, o_j \leq o_m$ the simultaneous invariants that are independent of the homogeneous moments and to each other using the algorithm by Langbein and Hagen [3]. We provide the overcomplete set in the appendix up to rank 6 in 2D and up to rank 4 in 3D.

Please remember that the overcomplete set is not a basis because the simultaneous invariants are not mutually independent but only independent within each pair o_i, o_j. Comparing Theorems 2 and 4 to Lemmata 5 and 9 shows that the number of elements of the overcomplete set is larger than the number of elements of a basis.

Then, to compose the flexible bases, we start with the overcomplete set and kick out all simultaneous invariants that do not contain the chosen non-zero moments of order o_0. Theorems 3 and 5 prove that this method indeed produces the correct number of independent invariants.

Now we will discuss how to select o_0 for a given pattern. To make the basis robust, it should use low order moments rather than higher order moments and avoid moments that are close to zero. We measure the magnitude of a moment tensor through the average magnitude of its entries

$$\|{}^oM\| = \tfrac{1}{n+m+o} \sum_{i_1 \ldots i_n, j_1 \ldots j_m, k_1 \ldots k_o = 1}^{3} |{}^oM^{i_1 \ldots i_n k_1 \ldots k_o}_{j_1 \ldots j_m}| \tag{44}$$

and during runtime, we select o_0 as the lowest order moment tensor satisfying $o + r_f \geq 1$ whose norm is above average, i.e.,

$$o_0 = \operatorname*{argmin}_{o \leq o_m, r = o + r_f > 1} \|{}^oM\| > \tfrac{1}{o_m+1} \sum_{o=0}^{o_m} \|{}^oM\|. \tag{45}$$

Then, the basis is given through all precomputed homgeneous plus simultaneous invariants of orders o_0, o, where $o_0 \neq o = 0, \dots, o_m$.

For the actual pattern matching, we compute the moments of the pattern and the field, select the significantly non-zero moment o_0 of the pattern, evaluate the corresponding basis, take the r-th root of each element with r being the rank of the tensor product it consists of to balance the contribution between different ranks, and use the reciprocal of the Euclidean distance of the descriptor vector as similarity. Please note that the Euclidean distance is not necessarily the optimal measures of similarity, but many others are possible, for example the Mahalanobis distance [30].

5.5. 2D Example of flexibility

In this section, we will demonstrate that our algorithm applied to the example pattern from Section 4.1 is complete. Up to order 3 in 2D, the homogeneous invariants are:

$$\begin{aligned}
{}^0M &= M\\
{}^1M^2{}_{(0,1)} &= M_0^2 + M_1^2\\
{}^2M_{(0,1)} &= M_{00} + M_{11}\\
{}^2M^2{}_{(0,2),(1,3)} &= M_{00}^2 + 2M_{01}^2 + M_{11}^2\\
{}^3M^2{}_{(0,1),(2,3),(4,5)} &= M_{000}^2 + M_{001}^2 + M_{011}^2 + M_{111}^2\\
&\quad + 2M_{000}M_{011} + 2M_{001}M_{111}\\
{}^3M^2{}_{(0,3),(1,4),(2,5)} &= M_{000}^2 + 3M_{001}^2 + 3M_{011}^2 + M_{111}^2\\
{}^3M^4{}_{(0,3),(1,6),(4,7),(2,9),(5,10),(8,11)} &= M_{000}^4 + 3M_{001}^4 + 3M_{011}^4 + M_{111}^4\\
&\quad + 4M_{000}M_{011}^3 + 6M_{000}^2M_{001}^2\\
&\quad + 12M_{001}^2M_{011}^2 + 4M_{001}^3M_{111}\\
&\quad + 6M_{011}^2M_{111}^2 + 12M_{000}M_{001}^2M_{011}\\
&\quad + 12M_{001}M_{011}^2M_{111}.
\end{aligned} \tag{46}$$

Since the non-zero moments are M_{11} and M_{000}, the algorithm selects the lower rank $o_0 = 2$. The simultaneous invariants that remain after removing all that do not contain order 2 are as follows.

$$\begin{aligned}
{}^1M^{22}M_{(0,2),(1,3)} &= M_0^2M_{00} + M_1^2M_{11} + 2M_0M_1M_{01}\\
{}^2M^{13}M^2{}_{(0,2),(1,3),(4,5),(6,7)} &= M_{00}M_{000}^2 + M_{00}M_{001}^2 + M_{11}M_{011}^2\\
&\quad + M_{11}M_{111}^2 + M_{00}M_{000}M_{011}\\
&\quad + M_{00}M_{001}M_{111} + 2M_{01}M_{000}M_{001}\\
&\quad + 4M_{01}M_{001}M_{011} + 2M_{01}M_{011}M_{111}\\
&\quad + M_{11}M_{000}M_{011} + M_{11}M_{001}M_{111}.
\end{aligned} \tag{47}$$

The basis comprises the homogeneous (46) and simultaneous invariants (47). They take the values

$$\begin{aligned}
&{}^0M = 0, \quad {}^2M^2_{(0,2),(1,3)} = 1, \quad {}^3M^2_{(0,1),(2,3),(4,5)} = 1,\\
&{}^1M^2_{(0,1)} = 0, \quad {}^3M^2_{(0,1),(2,3),(4,5)} = 1, \quad {}^1M^{22}M_{(0,2),(1,3)} = 0,\\
&{}^2M_{(0,1)} = 1, \quad {}^3M^2_{(0,3),(1,4),(2,5)} = 1, \quad {}^2M^{13}M^2_{(0,2),(1,3),(4,5),(6,7)} = 0.
\end{aligned} \tag{48}$$

Analogous to Flusser [6], we remove the one degree of freedom that refers to the rotational invariance by fixing one moment's degree of freedom. Without loss of generality, we select to set $M_{000} = 1$ so that we can keep the calculation simple. All correct values follow from straight calculation solving for $10 - 1 = 9$ unknowns in 9 equations. We will provide a sketch. With $M_{000} = 1$, it follows from the three 3rd order homogeneous invariants that $M_{001} = M_{011} = M_{111} = 0$. Inserting these values into the simultaneous invariant of orders 2 and 3 immediately gives $M_{00} = 0$, which leads to $M_{11} = 1, M_{01} = 0$ using the two 2nd order homogeneous invariants. Finally $M_0 = 0$ follows from the simultaneous invariant of orders 1 and 2, $M_1 = 0$ from 1st order homogeneous invariant, and $M = 0$ was clear from the start.

Especially, the flexible basis is able to discriminate the functions (7) and (10) from Fig. 2, because the simultaneous invariant of orders 2 and 3 differs with the prior sufficing ${}^2M^{13}M^2{}_{(0,2),(1,3),(4,5),(6,7)} = 0$ and the latter being 1.

5.6. 3D Example of flexibility

Analogously, the flexible basis is able to discriminate the two patterns from Section 4.2. For example, it contains the higher factor homogeneous invariant ${}^3M^4{}_{(0,1),(2,3),(4,6),(5,7),(8,9),(10,11)}$, which takes the value 27 for f_1 from Equation (14), but the value 11 for f_2. The full basis can be found in the appendix.

5.7. Exceptions

In all of our experiments using real data, we have never encountered a case where no such o_0 different from zero could be found. In theory, it can happen for two possible reasons though. (1) The pattern does not differ from zero for all moments up to o_m. In this case, we consider the function to be zero and therefore fully rotationally invariant. (2) We have the case of a 3D scalar field, $r_f = 0$, and the only non-zero tensor is ${}^1T$. This function is rotationally symmetric along one axis. The degrees of freedom of a rotation of this type of function are only two and either choice of o_0 works just fine.

In both cases, we can choose o_0 arbitrarily or use the full precomputed, overcomplete set to ensure that every function can be distinguished from the pattern.

Please note that the overcomplete set will always work and can be used for simplicity if performance is not an issue.

5.8. Size of the problem

The algorithm by Langbein and Hagen [3] is still a crucial component inside our algorithm to check for the independence of the invariants, but the systematic approach reduces the size of the problem in theory.

The original algorithm required triangulating matrices of size $n_i \times n_m$ with the number of moments $n_m = 2^{r_f}(o_m+1)(o_m+2)/2$ in 2D and $n + m = 3^{r_f}(o_m+1)(o_m+2)(o_m+3)/6$ in 3D. Now we know that we can decompose the problem into many smaller ones of sizes $n_m = 2^{r_f}(o+1)$ in 2D and $n_m = 3^{r_f}(o+1)(o+2)/2$ in 3D for the homogeneous invariants. In 2D, the problem for the simultaneous invariants disappears completely, because we know we need only one. In 3D, the matrices reduce to $n_m = 3^{r_f}((o_0+1)(o_0+2)+(o+1)(o+2))/2$. Also the number of potential candidates of invariants n_i to fill up the matrix rows is reduced because only tensor products with one or two different types of factors have to be taken into account.

In practice, for the orders that we computed, Langbein's basis could be found faster though. Since both algorithms terminate when the number of required invariants are found, the factor dominating the computation time is the number of invariants that actually get tested and their sizes. Langbein's algorithm is efficient w.r.t. this number because it sorts the candidates by the number of factors and will find enough small simultaneous invariants before having even to check the large homogeneous ones that are necessary to ensure flexibility. The times of the precomputation can be found in the appendix.

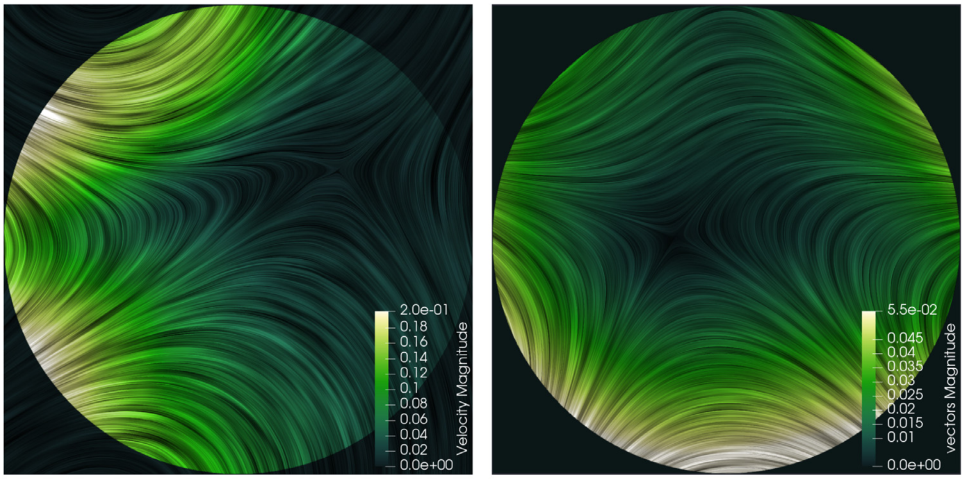

(a) The original pattern cut out from the dataset. (b) A pattern that does not appear in the data.

Fig. 4. The two patterns used for the experiment visualized through line integral convolution (LIC) [32] and velocity magnitude through color coding.

5.9. Implementation

We provide an open source implementation of the algorithms through the Visualization Toolkit VTK [31]. The moment invariants module (gitlab.kitware.com/vtk/MomentInvariants) is used for pattern detection and can be run using the method suggested by Bujack et al. [2], the method suggested by Langbein and Hagen [3], or the method suggested in this paper. The derivation of the independent homogeneous invariants is very time consuming for high ranks, which is why we separate it from the main pattern detection algorithm, where we use the hard-coded invariants.

6. Experiments

We will demonstrate the difference between the flexible basis and Langbein's basis on two real world datasets.

Please note that the two algorithms produce very similar results for most real world patterns. In order to show cases where they differ noticeably, we explicitly chose locations in the datasets that have a very small rank one component.

6.1. 2D Vector

Fig. 5 shows one timestep of a hydrodynamics simulation of a von Kármán vortex street. This flow behavior is the result of a laminar fluid being forced around an obstacle, which periodically sheds vortices in alternating orientation in its wake. We cut out a pattern with small first rank moments from the 2D vector-valued dataset, Fig. 4, rotate it, and let the algorithm look for it in the full dataset.

We can see in the top row of Fig. 5 that both bases, Langbein's and ours, have no problem detecting the correct location of

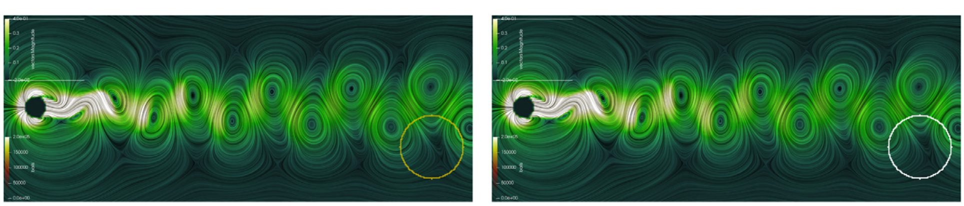

(a) Langbein invariants and existing pattern with maximum similarity of $148K$. (b) Flexible and existing pattern with maximum similarity of $508K$.

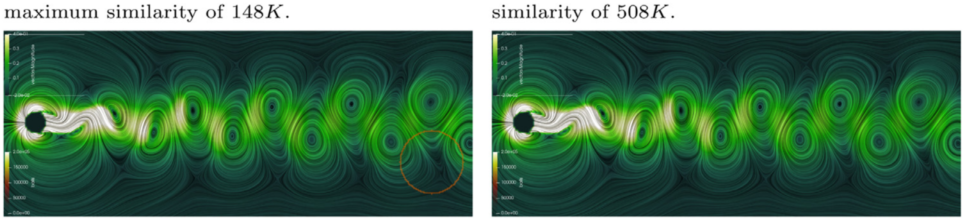

(c) Langbein invariants and non-existing pattern with maximum similarity of $112K$. (d) Flexible and non-existing pattern with maximum similarity of 62.

Fig. 5. Comparison of the pattern detection results on the velocity of a fluid dynamics simulation. The velocity field is visualized using LIC in green in the background. The similarity is color coded using the heated body map and transparency on top with 0 being fully transparent and $2e5$ being completely opaque. The algorithm by Langbein cannot distinguish the two patterns and returns approximately the same similarity for both, while our flexible algorithm detects the correct pattern about $10K$ times stronger than the wrong pattern. (For interpretation of the references to colour in this figure legend, the reader is referred to the web version of this article.)

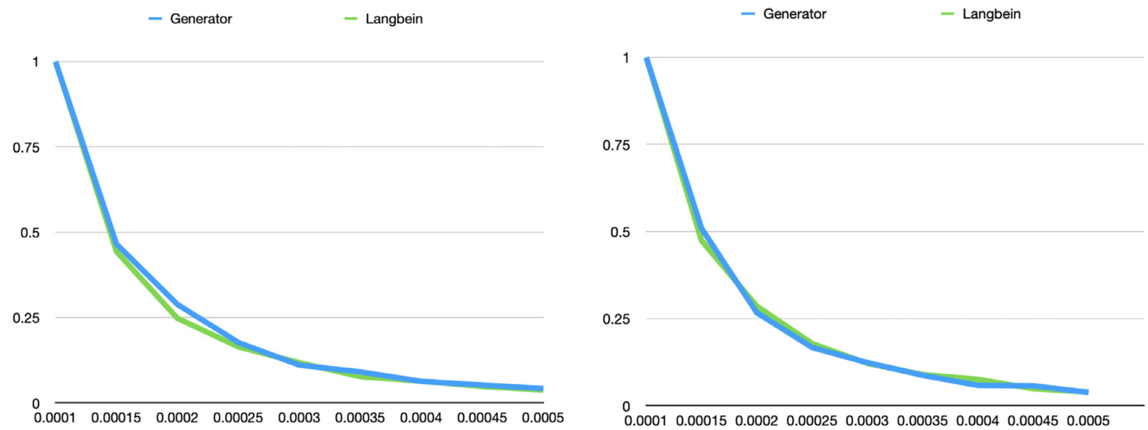

(a) The 2D vector values data from Figure 5. The signal to noise ratio drops from 17.8 to 11.8 .

(b) The 3D scalar values data from Figure 7a. The signal to noise ratio drops from 16.3 to 10.6 .

Fig. 6. Average normalized similarity of 10 randomly cut out patterns depending on added uniform noise in $[-1, 1]$ multiplied with the values on the x-axis shows that both bases behave similar in most cases.

the pattern independent of the new orientation. To demonstrate the difference in their behavior, we let them look for a different pattern, Fig. 4b, which does not occur in the dataset, but has the same homogeneous invariants as the cut out pattern, Fig. 4a. Please note the different velocity magnitudes. We see that Langbein's basis cannot discriminate the two patterns, while our flexible basis clearly does in the lower row of Fig. 5.

To show that both algorithms behave comparably in most settings, we cut out 10 patterns randomly selected from the dataset and compare the similarity by which each basis detects them for rank 3 when they get distorted with increasing amounts of uniform random noise. We normalize the similarity with noise in $10^{-3}[-1, 1]$ to one so that the graphs of the different bases are directly comparable. The average results of 500 repetitions can be found in Fig. 6.

6.2. 3D Scalar

For this example, we use the velocity magnitude of one timestep of the homogeneous buoyancy driven turbulence dataset [33,34]. It is produced by Los Alamos National Laboratory's Direct Numerical Simulation (DNS) code and is available at Johns Hopkins Turbulence Database [35,36]. For this simulation, two fluids are initialized randomly at rest and later mix due to gravity and differential buoyancy forces.

We cut out a pattern with small moments of orders 1 and 2 from the 3D scalar-valued dataset, as shown in Fig. 7. Then, analogously to the example in Section 4.2, we construct a false pattern by replacing the value of M_{012} with its negative. We rotate the patterns, and let the algorithms look for them in the original dataset. Fig. 9 compares the results of the Langbein basis and the flexible basis for the reconstructed pattern, whose moments up to order 3 coincide with one location in the data, and the false pattern, differing in the sign of $M_{012} = -0.0005$. The little outlined cube shows the correct location of the cut out pattern, which is correctly detected by both algorithms. The algorithm by Langbein has a hard time distinguishing the two patterns even though the first order moments do not vanish completely, but are in the range of 0.0005, same as M_{012} and only one order of magnitude smaller than the largest moment of this pattern. In contrast to that, the flexible basis detects the correct pattern about 30 times stronger than the wrong pattern.

As mentioned before, the degenerate cases in which moments vanish completely are rare in real world data. In normal settings, both bases behave similar, Fig. 6(b).

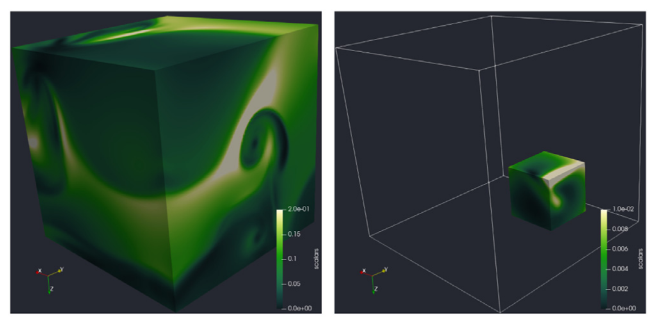

(a) The dataset.

(b) The pattern located in the data.

Fig. 7. The dataset and pattern visualized using color coding on the surface.

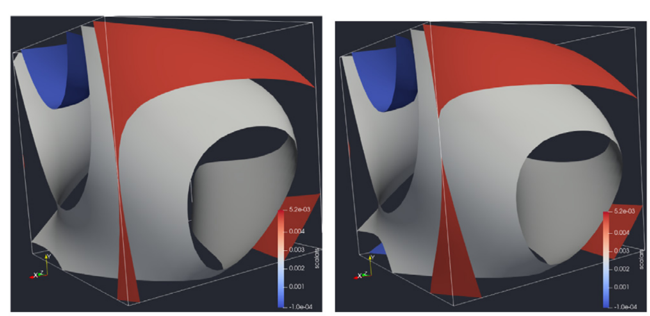

(a) The pattern from the dataset.

(b) A pattern that does not appear in the data.

Fig. 8. The patterns used for the 3D experiment visualized with nested isosurfaces.

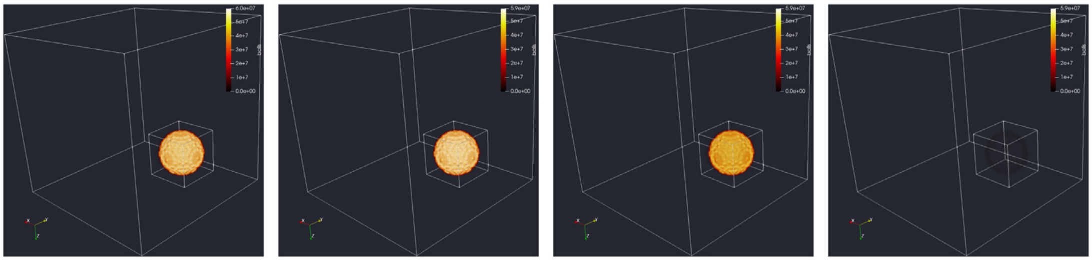

(a) Langbein and existing pattern with maximum similarity of $59M$. (b) Flexible and existing pattern with maximum similarity of $59M$. (c) Langbein and non-existing pattern with max. similarity of $53M$. (d) Flexible and non-existing pattern with max. similarity of $2M$.

Fig. 9. Comparison of the pattern detection results on the velocity magnitude of the DNS simulation visualized with volume rendering. The similarity is color coded using the heated body map and transparency on top with 0 being fully transparent and 59*M* being fully opaque.

7. Discussion and conclusion

We have presented a systematic approach to find bases of moment invariants with respect to orthogonal transformations using the generator method for scalar, vector, and tensor fields in 2D and 3D.

Provided that our conjecture holds, i.e., that the set of all tensor contractions is complete, we showed that it is always possible to construct a basis using all homogeneous invariants and simultaneous invariants with no more than two different moment tensors and with one of the factors fixed per pattern.

This result is very important from a theoretical perspective because it reveals the structural similarity between the 3D generator approach and the first complete and independent 2D generator approach for scalar fields by Flusser [6], which also uses products of tensors of only two different orders. It also reveals a stronger than so far expected similarity to the 3D normalization approach [2], which also used one fixed normalizer, i.e., two different factors. The normalization approach and the generator approach have their advantages and disadvantages. We hope that an optimal basis can be constructed when we understand how to express one through the other [4] and consider the results of this work a step in the right direction.

The implications are also of a practical nature. Instead of checking for independence across all orders, we are able to decompose the problem into many smaller ones, which can be solved independent of each other. Further, the property that the needed simultaneous invariants can be formed with one of the factors fixed allows for a flexible algorithm that is always fully discriminative, independent of the shape of the input pattern.

We would like to point out though that vanishing moments occur far less in patterns cut out from real world data than for analytical patterns, which makes Langbein's basis work reliable in most of these cases. For a normal distribution of moments, it runs faster because it makes use of invariants from moment products of lower order and with fewer factors.

Declaration of Competing Interest

The authors declare that they have no known competing financial interests or personal relationships that could have appeared to influence the work reported in this paper.

Acknowlgedgments

This work has been supported by the Czech Science Foundation under the grants No. GA18-07247S and GA21-03921S and by the Praemium Academiae.

Supplementary material

Supplementary material associated with this article can be found, in the online version, at doi:10.1016/j.patcog.2021.108313

References

[1] J. Flusser, B. Zitova, T. Suk, 2D And 3D Image Analysis by Moments, John Wiley & Sons, 2016.
[2] R. Bujack, H. Hagen, Moment invariants for multi-dimensional data, in: E. Ozerslan, T. Schultz, I. Hotz (Eds.), Modelling, Analysis, and Visualization of Anisotropy, Mathematica and Visualization, Springer Basel AG, 2017.
[3] M. Langbein, H. Hagen, A generalization of moment invariants on 2d vector fields to tensor fields of arbitrary order and dimension, in: International Symposium on Visual Computing, Springer, 2009, pp. 1151–1160.
[4] R. Bujack, J. Flusser, Flexible moment invariant bases for 2D scalar and vector fields, in: Proceedings of International Conference in Central Europe on Computer Graphics, Visualization and Computer Vision (WSCG), 2017, pp. 11–20.
[5] M.-K. Hu, Visual pattern recognition by moment invariants, IRE Trans. Inf. Theory 8 (2) (1962) 179–187.
[6] J. Flusser, On the independence of rotation moment invariants, Pattern Recognit 33 (9) (2000) 1405–1410.
[7] J. Flusser, On the inverse problem of rotation moment invariants, Pattern Recognit 35 (2002) 3015–3017.
[8] M. Schlemmer, M. Heringer, F. Morr, I. Hotz, M. Hering-Bertram, C. Garth, W. Kollmann, B. Hamann, H. Hagen, Moment invariants for the analysis of 2D flow fields, IEEE Trans Vis Comput Graph 13 (6) (2007) 1743–1750.
[9] M. Schlemmer, I. Hotz, B. Hamann, H. Hagen, Comparative visualization of two-dimensional flow data using moment invariants, in: Proceedings of Vision, Modeling, and Visualization (VMV'09), 1, 2009, pp. 255–264.
[10] R. Bujack, I. Hotz, G. Scheuermann, E. Hitzer, Moment invariants for 2D flow fields using normalization, in: IEEE Pacific Visualization Symposium, PacificVis 2014 in Yokohama, Japan, 2014, pp. 41–48.
[11] C. Lo, H. Don, 3-D Moment forms: their construction and application to object identification and positioning, IEEE Trans. Pattern Anal. Mach. Intell. 11 (10) (1989) 1053–1064, doi:10.1109/34.42836.
[12] G. Burel, H. Henocq, 3D Invariants and their application to object recognition, Signal procesing 45 (1) (1995) 1–22.
[13] M. Kazhdan, T. Funkhouser, S. Rusinkiewicz, Rotation invariant spherical harmonic representation of 3D shape descriptors, Symposium on Geometry Processing, 2003.
[14] N. Canterakis, Complete moment invariants and pose determination for orthogonal transformations of 3D objects, in: Mustererkennung 1996, 18. DAGM Symposium, Informatik aktuell, Springer, 1996, pp. 339–350.
[15] T. Suk, J. Flusser, J. Boldyš, 3D rotation invariants by complex moments, Pattern Recognit 48 (11) (2015) 3516–3526.
[16] H. Dirilten, T.G. Newman, Pattern matching under affine transformations, Computers, IEEE Transactions on 100 (3) (1977) 314–317.
[17] Z. Pinjo, D. Cyganski, J.A. Orr, Determination of 3-D object orientation from projections, Pattern Recognit Lett 3 (5) (1985) 351–356, doi:10.1016/0167-8655(85)90067-4.
[18] D. Cyganski, J.A. Orr, Applications of tensor theory to object recognition and orientation determination, IEEE Trans. Pattern Anal. Mach. Intell. PAMI-7 (6) (1985) 662–673, doi:10.1109/TPAMI.1985.4767722.
[19] D. Cyganski, S.J. Kreda, J.A. Orr, Solving for the general linear transformation relating 3-d objects from the minimum moments, in: 1988 Robotics Conferences, International Society for Optics and Photonics, 1989, pp. 204–211.
[20] T. Suk, J. Flusser, Tensor method for constructing 3D moment invariants, in: Computer Analysis of Images and Patterns, in: Lecture Notes in Computer Science, 6855, Springer Berlin, Heidelberg, 2011, pp. 212–219.

[21] M.S. Hickman, Geometric moments and their invariants, J Math Imaging Vis 44 (3) (2012) 223–235.
[22] Y. Gur, C.R. Johnson, Generalized hardi invariants by method of tensor contraction, in: 2014 IEEE 11th international symposium on biomedical imaging (ISBI), IEEE, 2014, pp. 718–721.
[23] B. Xiao, L. Li, Y. Li, W. Li, G. Wang, Image analysis by fractional-order orthogonal moments, Inf Sci (Ny) 382 (2017) 135–149.
[24] B. Xiao, J. Luo, X. Bi, W. Li, B. Chen, Fractional discrete Tchebyshev moments and their applications in image encryption and watermarking, Inf Sci (Ny) 516 (2020) 545–559.
[25] L. Florack, B.T.H. Romeny, J. Koenderink, M. Viergever, Cartesian differential invariants in scale-space, J Math Imaging Vis 3 (4) (1993) 327–348.
[26] L. Florack, B.T.H. Romeny, J.J. Koenderink, M.A. Viergever, General intensity transformations and differential invariants, J Math Imaging Vis 4 (2) (1994) 171–187.
[27] T.H. Reiss, The revised fundamental theorem of moment invariants, IEEE Trans Pattern Anal Mach Intell 13 (8) (1991) 830–834.
[28] R. Bowen, C. Wang, Introduction to Vectors and Tensors, Dover books on mathematics, Dover Publications, 2008.
[29] P. Grinfeld, Introduction to Tensor Analysis and the Calculus of Moving Surfaces, Springer New York, 2013.
[30] M. Langbein, Higher Order Moment Invariants and their Applications, Technical University Kaiserslautern, 2014 Ph.D. Dissertation.
[31] The Visualization Toolkit User's Guide, Kitware, Inc., 2003.
[32] B. Cabral, L.C. Leedom, Imaging vector fields using line integral convolution, in: Proceedings of the 20th annual conference on Computer graphics and interactive techniques, in: SIGGRAPH '93, ACM, 1993, pp. 263–270, doi:10.1145/166117.166151.
[33] Johns Hopkins Turbulence Databases, Homogeneous Buoyancy Driven Turbulence Data Set, http://turbulence.pha.jhu.edu/Homogeneous_buoyancy_driven_turbulence.aspx, Accessed: 2018-06-14.
[34] D. Livescu, C. Canada, K. Kanov, R. Burns, J. Pulido, et al., Homogeneous buoyancy driven turbulence data set, 2015.
[35] E. Perlman, R. Burns, Y. Li, C. Meneveau, Data exploration of turbulence simulations using a database cluster, in: Proceedings of the 2007 ACM/IEEE conference on Supercomputing, ACM, 2007, p. 23.
[36] Y. Li, E. Perlman, M. Wan, Y. Yang, C. Meneveau, R. Burns, S. Chen, A. Szalay, G. Eyink, A public turbulence database cluster and applications to study lagrangian evolution of velocity increments in turbulence, J. Turbul. (9) (2008) N31.

Roxana Bujack graduated as M.Sc. in math- ematics at Leipzig University in Germany in 2010. Then, she received her B.Sc. and her Ph.D. in computer science in the Image and Signal Processing Group at Leipzig Univer- sity. She worked as a postdoctoral researcher at IDAV at the University of California, Davis in the USA and at the Computer Graphics and HCI Group at the Technical University Kaiserslautern. Currently, she is a staff sci- entist in the Data Science at Scale Team at Los Alamos National Laboratory. Her re- search interests include visualization, pattern recognition, vector fields, moment invariants, data science, HPC, Lagrangian ow represen- tations, and color theory.

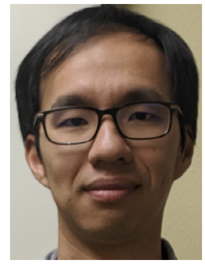

Xinhua Zhang received a M.Sc. in computer science at Shanghai Jiao Tong University in China and a M.Sc. in electrical and computer engineering at Georgia Institute of Technology in 2012. He currently is a Ph.D student at the University of New Mexico working on Eu- clidean invariance and equivariance. He joined Los Alamos National Laboratory in 2018 as a permanent student. His research interests in- volve pattern detection, computer vision and computational neural science.

Tomas Suk received the M.Sc. degree in electrical engineering from the Czech Tech- nical University, Faculty of Electrical Engi- neering, Prague, Czech Republic, in 1987 and the Ph.D degree in computer science from the Czechoslovak Academy of Sciences in 1992. Since 1991 he has been a researcher with the Institute of Information Theory and Automa- tion, Czech Academy of Sciences, Prague. He has authored 15 journal papers and more than 30 conference papers. Tomas Suk's research interests include digital image processing, pat- tern recognition, image filtering, invariant fea- tures, moment-based and point-based invari- ants, spatial transformations of images, and applications in remote sensing, astronomy, botany, medicine, and computer vision. In 2002 Tomas Suk received the Otto Wichterle Premium of the Czech Academy of Sciences for excellent young scientists.

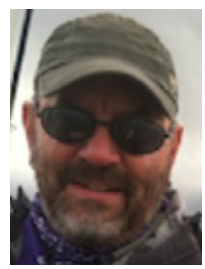

David H. Rogers joined LANL in 2013, af- ter a decade of leading the Scalable Analysis and Visualization Team at Sandia National Labs, where he was instrumental in bringing in-situ analysis and visualization into production. He now focuses on interactive web-based analysis tools that integrate design, scalable analytics and principles of cognitive science to promote scientific discovery. Prior to working on large scale data analysis, David worked at DreamWorks Feature animation, writing and managing production software. He has degrees in Computer Science, Architecture (buildings, not computers), and an MFA in Writing for Children.